Fiber twisting

DOI: 10.1002/smll.200600368

Strong Carbon-Nanotube Fibers Spun from Long Carbon-Nanotube Arrays**

*Xiefei Zhang, Qingwen Li, Yi Tu, Yuan Li, James Y. Coulter, Lianxi Zheng, Yonghao Zhao, Qianxi Jia, Dean E. Peterson, and Yuntian Zhu**

The superior mechanical properties of carbon nanotubes (CNTs) mean they have been regarded as a new material with the potential to revolutionize and enable many advanced technologies. CNTs have extremely high tensile strength ($\approx$150 GPa),[1] high modulus ($\approx$1 TPa),[2] large aspect ratio, low density, good chemical and environmental stability, and high thermal and electrical conductivity. These superior and unique properties make CNTs very attractive for many structural applications such as aerospace structures, body armors, and sporting goods. Early studies of CNT-reinforced nanocomposites showed that CNTs were effective fillers to enhance the mechanical properties of polymer matrices,[3,4] but the reinforcement was limited by the quality of dispersion, CNT alignment, and load-transfer efficiency between the CNT and the matrix. The full reinforcement potential of CNTs has not yet been utilized in CNT composites.

It has been a challenge to make macroscale CNT structures and to fully utilize the outstanding mechanical properties of CNTs. The first macroscale CNT structure was in the form of a film called buckypaper, which displayed relatively high electrical and thermal conductivity, but low mechanical properties.[5] For the purpose of obtaining superior mechanical performance, researchers have recently focused on CNT fibers. The first CNT fiber was successfully prepared through spinning a CNT homogeneous dispersion into a polyvinyl alcohol (PVA) coagulation bath.[6] This approach was modified by Baughman's group to make single-walled (SW) CNT composite fibers with very high strength.[7,8] The major issues with this approach include a relatively high fraction of remaining polymer volume and short individual CNTs, which limits the fiber's strength, electrical and thermal conductivity.[9]

[*] Dr. X. Zhang, Dr. Q. Li, Y. Li, J. Y. Coulter, Dr. L. Zheng, Dr. Y. Zhao, Dr. Q. Jia, Dr. D. E. Peterson, Dr. Y. Zhu
Materials Physics and Application Division
Los Alamos National Laboratory
Los Alamos, NM 87545 (USA)
Fax: (+1) 505-663-5550
E-mail: yzhu@lanl.gov
Dr. Y. Tu
First Nano, a Division of CVD Equipment Corporation
1860 Smithtown Ave, Ronkonkoma, NY 11779 (USA)

[**] This work was supported by the Laboratory Directed Research and Development (LDRD) program office of Los Alamos National Laboratory.

Recently, new approaches have been reported in which pure CNT fibers were spun without a matrix. For example, pure CNT fibers were spun from a CNT-fuming sulfuric acid solution.[10] A continuous multi-walled (MW) CNT yarn was pulled from a high-quality array without twisting.[11] SWCNT fibers were spun from an aerogel in the chemical vapor deposition synthesis zone,[12,13] and MWCNT fibers were spun from CNT arrays.[14,15] These CNT fibers usually have a strength of $\leq$1.5 GPa and a Young's modulus of $\leq$30 GPa. Here, we report the spinning of CNT fibers from relatively long CNT arrays (0.65 mm). The influence of post-spin twisting on the mechanical performance of these fibers is also discussed.

Figure 1a shows a scanning electron microscopy (SEM) image of the 0.65-mm CNT array, which is synthesized by

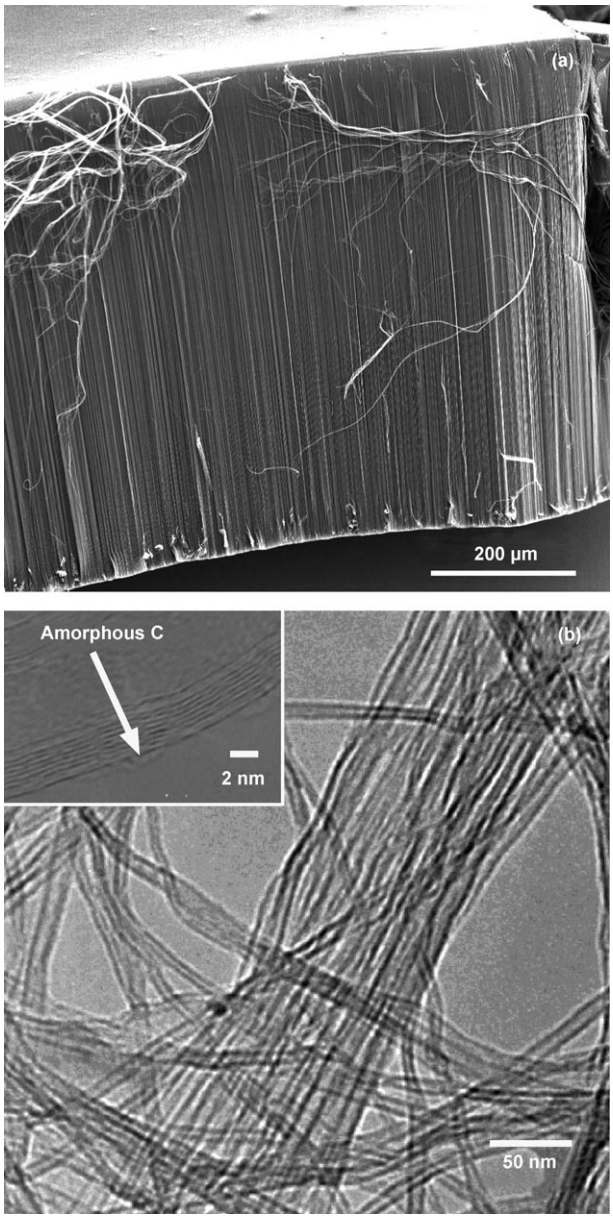

Figure 1. Characterization of a long CNT array: a) SEM image showing a well-aligned CNT array with a length of 0.65 mm. b) Transmission electron microscopy (TEM) image of individual CNTs.

CVD and used for fiber spinning. High-resolution electron microscopy (HREM) reveals that CNTs in the array are multi-walled with an average diameter of around 10 nm (see Figure 1b). HREM observations also reveal that the CNT array is relatively clean with very little amorphous carbon (see Figure 1b inset). To check the array quality and spinnability, we carefully pulled ribbons from the CNT array with a pair of sharp tweezers and investigated it using SEM.

Figure 2a and b shows the SEM images of a CNT ribbon that was initially pulled from the CNT array before spinning. The good ribbon continuity shown in Figure 2a and b is important for fiber spinning, and this continuity is likely associated with CNT-quality characteristics, such as alignment, purity, density, and so on.[11,14] Figure 2c is the SEM image of an as-spun fiber. As shown, the as-spun fiber is relatively loose with noticeable spaces between CNTs or CNT bundles, and the twist angle, defined as the angle between the longitudinal direction of individual CNTs and the axis of the CNT fiber, is small. As shown later, such a structure does not lead to strong CNT fibers.

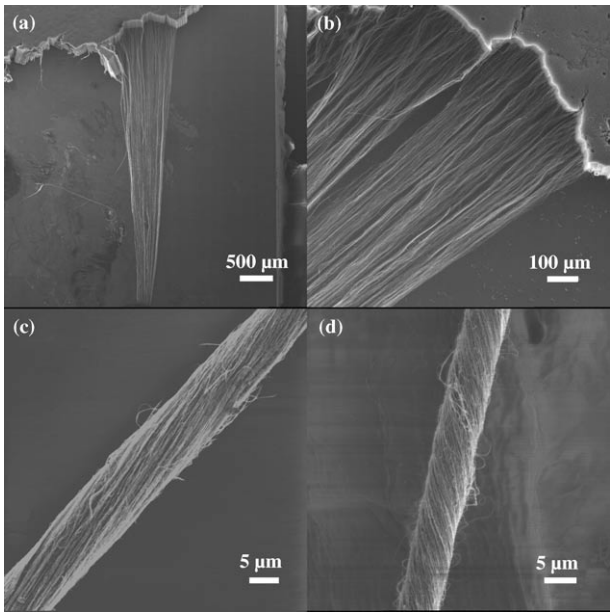

Figure 2. SEM images of CNT ribbons and fibers: a, b) CNT ribbon initiated from a CNT array for spinning; c) as-spun CNT fiber; d) the same fiber after post-spin twisting.

To improve the mechanical properties of the CNT fiber, post-spin twisting was carried out on as-spun fibers. This process gave the CNT fiber a higher density (smaller diameter) and larger twist angle (as shown in Figure 2d). After post twisting, the estimated twist angles of outer-layer CNTs increased from 10° to 21°. Comparison of Figure 2c and d reveals that the post-spin twist decreases the diameter of the CNT fibers by about 30% from 10 to 7 μm. The post-spin twisting brings the CNTs in closer contact to each other and therefore enhances the van der Waals forces and friction, which improves the load transfer between the CNTs. In other words, it improves the CNT fiber in two aspects: better load transfer and higher density, both of which will improve the strength of the CNT fiber.

To determine the array-length effect on the mechanical strength of the fibers, we spun fibers with comparable diameters (approximately 4 μm) from arrays of 300, 500, and 650 μm in length and measured the strengths with a Rheometrics solids analyzer. The tensile strengths for those as-spun fibers are 0.32, 0.56, and 0.85 GPa, respectively (as shown in Figure 3a). In general, the tensile strength of a twisted fiber can be described by the following equation:[14]

$$\frac{\delta_f}{\delta_{CNT}} \approx \cos\alpha[1 - (k \operatorname{cosec}\alpha)] \quad (1)$$

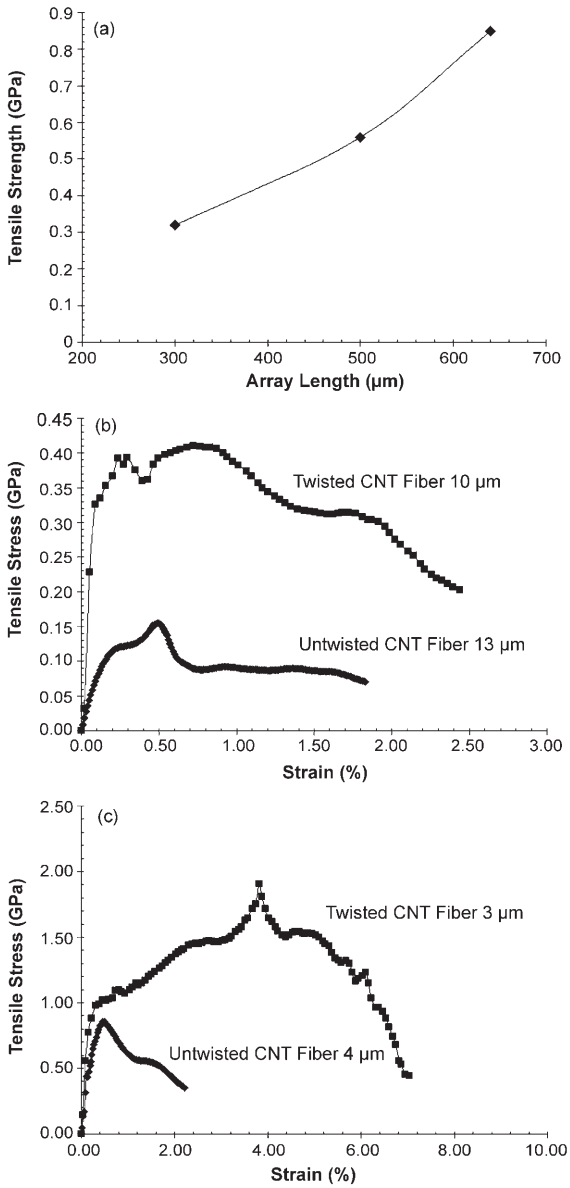

Figure 3. Mechanical behavior of CNT fibers: a) tensile strengths of as-spun fibers from arrays of 300, 500, and 650 μm in length, respectively; b) as-spun and post-twisted large-diameter CNT fibers spun from a 650-μm array; c) as-spun and post-twisted small-diameter CNT fibers spun from a 650-μm array. All the samples have a gauge length of 10 mm and were tested at a displacement rate of 0.05 mm s^{-1}.

where δ_f and δ_{CNT} are the tensile strengths of the twisted fiber and the CNT, respectively; α is the twist angle, and $k = (dQ/\mu)^{1/2}/3L$. Here, d is the CNT diameter, L is the CNT length, μ is the friction coefficient between CNTs, and Q is the CNT migration length. Equation (1) indicates that the fiber strength increases with increasing CNT length and decreasing CNT diameter. Also, it was shown in previous studies that the yarn strength was affected by fiber strength, fiber length, and fiber size.[16] Interfiber friction can be a dominant factor in determining the tensile properties of yarn under certain conditions. Friction- and yarn-strength studies showed that moderate changes in the interfiber friction can produce large changes in yarn strength.[17] In our work, individual CNTs or CNT bundles can be regarded as fibers, and CNT fibers can be regarded as yarn in textile industrial terminology. Longer nanotubes will lead to a higher friction force at the nanotube interfaces. Moreover, longer nanotubes will introduce fewer mechanical defects—the ends of nanotubes can be regarded as defects—per unit fiber length. Therefore, longer nanotubes definitely contribute positively to the strength of CNT fibers.

For our study, we only continued with the array that had the best mechanical properties and we report on the process, structure, and property. Two batches of CNT fibers were spun from a 650-μm array with different diameters of 13 and 4 μm. Some of those fibers underwent post-spin twisting. As listed in Table 1, the smaller-diameter fibers have better mechanical properties in both the as-spun and the post-spin-twisted states. For example, the 4-μm as-spun fiber has a tensile strength of 0.85 GPa, which is much higher than 0.17 GPa, the tensile strength of the 13-μm as-spun fiber. There are several possible reasons for the observed size effect. First, similar to advanced ceramic fibers such as Nicalon fiber,[18] the strength of the CNT yarn is largely controlled by the size of defects in the yarn. A yarn with a larger diameter has a higher probability of containing larger defects, and consequently lower strength. Second, there exists an optimal twisting angle that yields the best strength. It is well known that the twisting angle of individual nanotubes varies from the yarn center to the surface. A yarn with a larger diameter may have a smaller fraction of CNTs that have a near-optimal twisting angle, which leads to lower yarn strength. Fiber-diameter-related strength-limiting defects have also been discussed in a previous report.[19] There could also be other reasons that contribute to the size effect. More studies are underway to investigate this issue.

Table 1. Typical mechanical properties of CNT fibers spun from a 0.65-mm CNT array.

Processing state	Diameter [μm]	Tensile strength [GPa]	Young's modulus [GPa]	Elongation to failure [%]
As-spun	4	0.85	275	2.21
	13	0.17	89	1.83
Post-spin twisted	3	1.91	330	7.02
	10	0.41	241	2.43

The post-spin twisting increased the density of the CNT fibers, as evidenced by the diameter shrinkage shown in Figure 2 and listed in Table 1. This in turn significantly increased the strengths of the CNT fibers, which was due to both the decrease in diameter and increase in the load-carrying capacity of the CNT fibers. The 13-μm as-spun fiber decreased in diameter by 23% to 10 μm after the post-spin twisting, and had a 43% increased load-carrying capacity. This led to a 140% increase in strength from 0.17 GPa to 0.41 GPa. Similarly, the post-spin twisting decreased the diameter of the 4-μm as-spun fiber by 25% and increased its load-carrying capacity by 26%, which led to a 125% increase in strength from 0.85 GPa to 1.91 GPa. In addition, as listed in Table 1, the post-spin twisting also increased the elongation-to-failure values and the Young's moduli of the CNT fibers.

The increase in load capacity by post-spin twisting is caused by two factors: stronger inter-CNT interaction and higher radial-compressive stress. The stronger inter-CNT interactions result from the closer inter-CNT distance after the post-spin twisting, which increases the van der Waals force along individual CNTs. The higher radial-compressive stress increases the frictional stress during the fiber-tensile testing. In addition, during tensile testing, the radial-compressive stress increases with the tensile stress, which increases the effectiveness of load transfer via mechanical interlocking between the CNTs. These analyses are consistent with relevant studies reported in the literature. For example, a model predicted the existence of compressive stress in the radial direction of twisted yarns,[20] and the increase of the interfilament friction and shear modulus. Another previous study pointed out that in twisted structures the effective load transfer via frictional force can quickly build up stresses along the ends of broken filaments and consequently improve the strength of the twisted structure.[21]

As shown in Figure 3b and c, the strain–stress curves do not progress smoothly under tension. Also, the CNT fibers do not break in an abrupt manner. The SEM image (Figure 4) of a fractured fiber end suggests possible sliding between CNT strands during the failure process. Otherwise, a smooth fractured surface should have been observed instead. From this experimental, we propose the following reasonable mechanism for the mechanical behavior of the CNT fibers. Under a tensile load, some CNTs in the fiber carry more load than slack CNTs, and will break first under increasing load, which causes a stress dip. These broken CNTs will then slide against the unbroken CNTs and transfer the load onto the latter, which leads to a stress recovery and/or increase. More studies are underway to verify this hypothesis.

The larger elongation-to-failure value of post-spin twisted fibers can be explained by both the slippage of CNTs within the fibers and larger twisting, which is consistent with previous studies.[22] Also, previous theoretical and experimental studies indicated that twisting decreases the fiber modulus.[20] This is different from our observations. The discrepancy could be caused by the increase in fiber density in-

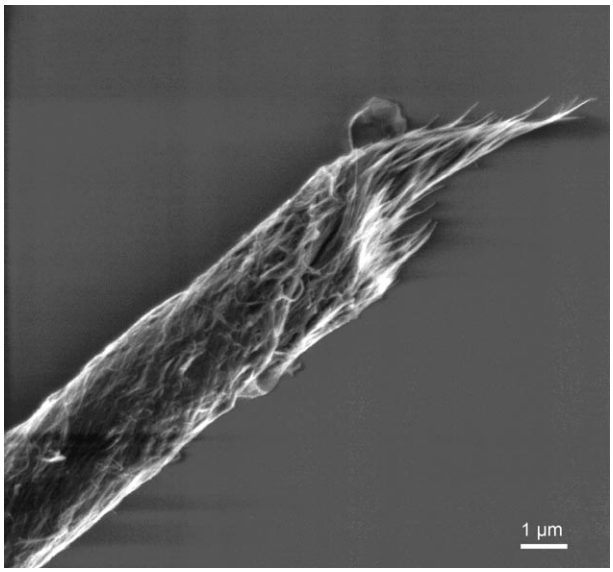

Figure 4. Fracture morphology of a CNT fiber.

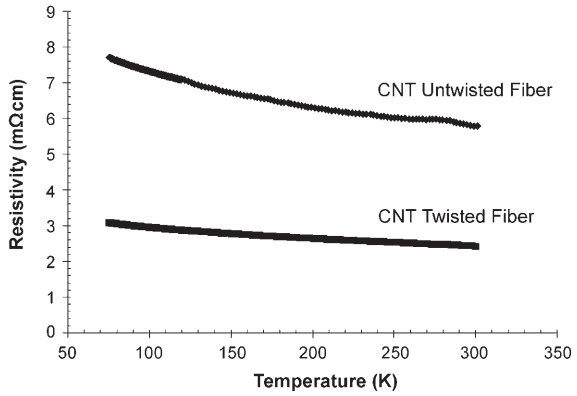

Figure 5. Resistivities as a function of temperature of as-spun and post-spin-twisted CNT fibers.

duced by the post-spin twisting. First, the twisting improves the CNT packing density, which consequently reduces the fiber cross-sectional area. This will in turn result in an increase in modulus. Second, the twisting will, to some extent, straighten wavy individual CNTs, leading to an increase in modulus. Third, larger twisting angles theoretically lead to a lower modulus.[23] The combination of these three factors led to the discrepancy between the ideal theoretical model and our experimental results. Similar phenomena were also observed in twisted polyacrylonitrile nanofiber yarn.[24]

The high strength coupled with high elongation-to-failure values makes our CNT fibers very tough. In other words, it takes a large amount of energy to break the CNT fibers. This energy can be calculated as the area under the stress–strain curve. The toughness values of those fibers range from 1.8×10^3 to 8.9×10^4 kJ m^{-3}. The observed superior toughness makes these CNT fibers attractive for many structural applications because they help to prevent catastrophic failure.

Figure 5 shows the resistivity as a function of temperature for as-spun and post-spin-twisted CNT fibers measured by the four-probe method. At room temperature, the resistivities of the as-spun and post-spin-twisted CNT fibers are 5.8 and 2.4 mΩcm, respectively, corresponding to electrical conductivities of 1.7 and 4.1×10^4 S m^{-1}, respectively, which is of the same order as those for bulk nanotube films and fibers.[5] The electrical conduction requires physical contact between CNTs. Post-spin twisting improved the conductivity by bringing CNTs into closer contact, which in turn explains the mechanical-properties improvement by stronger van der Waal forces and higher friction between tubes. The resistivity–temperature curve indicates typical semiconductive behavior, which implies that semiconducting CNTs dominate in these CNT fibers.

In summary, strong and stretchable fibers have been spun from 0.65-mm-long CNT arrays. After post-spin twisting, the strength and Young's modulus of the CNT fibers reached 1.91 GPa and 330 GPa, respectively. These superior mechanical properties of our CNT fibers are derived from the long individual CNTs in the CNT array as well as post-spin twisting. The post-spin twisting also improved the electrical conductivities of as-spun fibers by 140% from 1.7 S m^{-1} to 4.1×10^4 S m^{-1}. Based on these results, future work should focus on the synthesis of longer spinnable CNT arrays and optimization of the spinning process. In addition, incorporating a polymer matrix into the CNT fiber should also further improve the fiber strength.[25,26]

Experimental Section

Briefly, we grew a 0.65-mm-tall CNT array on a 1-nm-thick Fe film deposited on an Al_2O_3-coated Si substrate using ethylene as the carbon-source gas. The synthesis details of the CNT array will be reported in another paper.[27]

CNT fibers were spun from a CNT array using a spindle made of a microprobe. The microprobe spindle was mounted on a motor with adjustable rotation speed. The spinning process was monitored under an optical microscope. Silicon nitride particles (2 μm) were deposited onto the tip of the microprobe to increase its roughness, which is needed to initiate the spinning. CNT fibers were spun with a rotation speed in the range of 1500 to 2500 rpm and a drawing speed of about 5 cm min^{-1}. At first, a CNT ribbon was pulled off the array; the rotating microprobe was then moved to touch and entangle the CNT ribbon, after which the spindle moved away from the array at a constant linear speed, rotation rate, and desired angle with respect to the array. The as-spun fiber diameters are determined by the width of the initial ribbon. We spun each CNT fiber 20 cm long for easy handling. However, there should be no theoretical length limit in this spinning approach.

In the post-spin twisting process, a proper weight was hung on one end of a fiber to provide tension in the axial direction, while the other end of the fiber was attached to a rotator. The extent of further twisting depends on the twisting speed and duration. In the current study, a CNT fiber 5 cm long was typically twisted at a rotation rate of 500 rpm for 2 min.

HREM was carried out with a JEOL 3000F microscope. The mechanical properties of the CNT fibers were characterized by a Rheometrics solids analyzer RSAIII. The CNT fibers were mounted on paper tabs with a gauge length of 10 mm. The fiber diameter was measured using a laser-diffraction method. The extension speed was 0.05 mm s^{-1}.

Keywords:
arrays · carbon nanotubes · mechanical properties · nanofibers

[1] B. G. Demczyk, Y. M. Wang, J. Cunnings, M. Hetman, W. Han, A. Zettl, R. O. Ritchie, *Mater. Sci. Eng. A* **2002**, *334*, 173 – 178.
[2] M. F. Yu, B. S. Files, S. Arepalli, R. S. Ruoff, *Phys. Rev. Lett.* **2000**, *84*, 5552 – 5555.
[3] S. Kumar, T. D. Dang, F. E. Arnold, A. R. Bhattacharyya, B. G. Min, X. F. Zhang, R. A. Vaia, C. Park, W. W. Adams, R. H. Hauge, R. E. Smalley, S. Ramesh, P. A. Willis, *Macromolecules* **2002**, *35*, 9039 – 9043.
[4] G. D. Zhan, J. D. Kuntz, J. L. Wan, A. K. Mukherjee, *Nat. Mater.* **2003**, *2*, 38 – 42.
[5] X. F. Zhang, T. V. Sreekumar, T. Liu, S. Kumar, *J. Phys. Chem. B* **2004**, *108*, 16435 – 16440.
[6] B. Vigolo, A. Penicaud, C. Coulon, C. Sauder, R. Pailler, C. Journet, P. Bernier, P. Poulin, *Science* **2000**, *290*, 1331 – 1334.
[7] A. B. Dalton, S. Collins, E. Muñoz, J. M. Razal, V. H. Ebron, J. P. Ferraris, J. N. Coleman, B. G. Kim, R. H. Baughman, *Nature* **2003**, *423*, 703.
[8] G. Gu, M. Schmid, P. W. Chiu, A. Minett, J. Fraysse, G. T. Kim, S. Roth, M. Kozlov, E. Munoz, R. H. Baughman, *Nat. Mater.* **2003**, *2*, 316 – 319.
[9] M. E. Kozlov, R. C. Capps, W. M. Sampson, V. H. Ebron, J. P. Ferraris, R. H. Baughman, *Adv. Mater.* **2005**, *17*, 614 – 617.
[10] L. M. Ericson, H. Fan, H. Peng, V. A. Davis, W. Zhou, J. Sulpizio, Y. Wang, R. Booker, J. Vavro, C. Guthy, A. N. G. Parra-Vasquez, M. J. Kim, S. Ramesh, R. K. Saini, C. Kittrell, G. Lavin, H. Schmidt, W. W. Adam, W. E. Billups, M. Pasquali, W. F. Hwang, R. H. Hauge, J. E. Fisher, R. E. Smalley, *Science* **2004**, *305*, 1447 – 1450.
[11] K. Jiang, Q. Li, S. Fan, *Nature* **2002**, *419*, 801.
[12] Y. L. Li, I. A. Kinloch, A. H. Windle, *Science* **2004**, *304*, 276 – 278.
[13] M. Motta, Y. L. Li, I. Kinloch, A. H. Windle, *Nano Lett.* **2005**, *5*, 1529 – 1533.
[14] M. Zhang, K. R. Atkinson, R. H. Baughman, *Science* **2004**, *306*, 1358 – 1361.
[15] M. Zhang, S. Fang, A. A. Zakhidov, S. B. Lee, A. E. Aliev, C. D. Williams, K. R. Atkinson, R. H. Baughman, *Science* **2005**, *309*, 1215 – 1219.
[16] A. S. Elsourad, S. Worley, L. S. Smith, *Text. Res. J.* **1974**, *44*, 301 – 306.
[17] R. M. Broughton, Y. Elmogahzy, D. M. Hall, *Text. Res. J.* **1992**, *62*, 131 – 134.
[18] S. T. Taylor, Y. T. Zhu, W. R. Blumenthal, M. G. Stout, D. P. Butt, T. C. Lowe, *J. Mater. Sci.* **1998**, *33*, 1465 – 1473.
[19] L. W. Steenbakkers, H. D. Wagner, *J. Mater. Sci. Lett.* **1988**, *7*, 1209 – 1212.
[20] Y. Rao, R. J. Farris, *J. Appl. Polym. Sci.* **2000**, *77*, 1938 – 1949.
[21] N. Pan, *Ocean Conf. Rec. (IEEE)* **1996**, *1*, 138 – 143.
[22] N. K. Naik, V. Madhavan, *J. Strain Anal. Eng. Des.* **2000**, *35*, 83 – 91.
[23] R. B. Pipes, P. Hubert, *Compos. Sci. Technol.* **2002**, *62*, 419 – 428.
[24] S. F. Fennessey, R. Farris, *Polymer* **2004**, *45*, 4217 – 4225.
[25] M. I. Panhuis, A. Maiti, J. N. Coleman, A. B. Dalton, B. McCarthy, W. J. Blau, *AIP Conf. Proc.* **2001**, *591*, 497.
[26] X. Zhang, T. Liu, T. V. Sreekumar, S. Kumar, V. C. Moore, R. H. Hauge, R. E. Smalley, *Nano. Lett.* **2003**, *3*, 1285 – 1288.
[27] Q. W. Li, X. F. Zhang, R. F. Depaula, L. X. Zeng, Y. H. Zhao, L. Stan, T. G. Holesinger, P. N. Arendt, D. E. Peterson, Y. T. Zhu, *Adv. Mater.* **2006**, *18*, 3160.

Received: July 21, 2006

